Progress In Electromagnetics Research, Vol. 135, 231–244, 2013

MODELING RADIATED ELECTROMAGNETIC EMISSIONS OF ELECTRIC MOTORCYCLES IN TERMS OF DRIVING PROFILE USING MLP NEURAL NETWORKS

Ahmed M. Wefky, Felipe Espinosa*, Luis de Santiago, Alfredo Gardel, Pedro Revenga, and Miguel Martínez

Department of Electronics, University of Alcalá, Alcalá, Madrid, Spain

Abstract—Current automotive electromagnetic compatibility (EMC) standards do not discuss the effect of the driving profile on real traffic vehicular radiated emissions. This paper describes a modeling methodology to evaluate the radiated electromagnetic emissions of electric motorcycles in terms of the driving profile signals such as the vehicle velocity remotely controlled by means of a CAN bus. A time domain EMI measurement system has been used to measure the temporal evolution of the radiated emissions in a semi-anechoic chamber. The CAN bus noise has been reduced by means of adaptive frequency domain cancellation techniques. Experimental results demonstrate that there is a temporal relationship between the motorcycle velocity and the radiated emission power in some specific frequency ranges. A Multilayer Perceptron (MLP) neural model has been developed to estimate the radiated emissions power in terms of the motorcycle velocity. Details of the training and testing of the developed neural estimator are described.

1. INTRODUCTION

In the next 50 years, the global population is expected to increase from 6 billion to 10 billion and thus the number of vehicles is estimated to increase from 700 million to 2.5 billion. If all these vehicles are propelled by internal combustion engines, where will the oil come from? And where should the emissions be disseminated? Answers to these questions impose people to strive for sustainable road transportation for the 21st century [1]. In a world where energy conservation and

Received 25 October 2012, Accepted 17 December 2012, Scheduled 20 December 2012

* Corresponding author: Felipe Espinosa (espinosa@depeca.uah.es).

environment protection are growing concerns, the development of electric vehicles has achieved an accelerated pace.

There are serious EMC problems in electric vehicles. A systematic model to analyze conducted interferences of the electric drive system has been presented in [2]. EMC issues related to the integration of an electric drive system into a conventional passenger car were investigated in [3]. Implementation difficulties encountered when measuring radiated electric and magnetic field emissions of experimental electric vehicles in the range 9 KHz to 30 MHz were described in [4]. Some electromagnetic interference (EMI) measurements including electric as well as magnetic field in two electric cars and a bus have been presented in [5]. Methods to control EMI noise generated in electric vehicle drive systems were studied using an electric vehicle prototype in [6].

There are several published works related to noise cancellation techniques in the EMC field. A noise cancellation method for estimating a specific signal with the existence of background noise of non-Gaussian distribution was presented in [7]. Also, an SVD based noise-reduction technique to improve the accuracy of radar target recognition was introduced in [8]. Besides, A Hidden Markov Model based meter self-noise cancellation method for Electromagnetic measurements has been proposed in [9]. Furthermore, ambient noise cancelation in TDEMI measurements has been investigated and applied in [10]. Moreover, hardware implementation of a real-time FPGA-based ambient noise cancellation system for EMI measurements in time domain has been developed in [11].

Artificial neural networks (ANNs) have been exploited in different EMC problems such as detection and identification of vehicles based on their unintended radiated emissions [12], target discrimination [13, 14], calculation of multilayer magnetic shielding [15], estimating PCB configuration from EMI measurements [16], characterization and modeling of the susceptibility of integrated circuits to conducted electromagnetic disturbances [17], recognition and identification of radiated EMI for shielding apertures [18], prediction of electromagnetic field in metallic enclosures [19], adaptive beamforming [20, 21], PAD modeling [22], and detection of dielectric cylinders buried in a lossy half-space [23]. This paper takes advantage of MLP neural networks to model and estimate motorcycle's radiated emissions in terms of the registered velocity.

The Electronics Department at the University of Alcala (UAH), in collaboration with the Thermal Engines Group of the ETSII-UPM in Madrid and the Research Center for Environmental Energy and Technology (CIEMAT) in Madrid developed an electronic

measurement equipment to relate the driver activity, vehicle state and road conditions with vehicular emissions (gases and particles) in real traffic conditions [24]. This was the starting point to extend the study to radiated emissions of electrical vehicles in this work.

The rest of the paper is arranged as follows: Section 2 illustrates the motivation and context of this work. Section 3 points out the measurement methodology followed in this paper. Neural model development details are discussed in Section 4. Section 5 is devoted to experimental results. Finally the sixth section includes conclusions and future works.

2. DRIVING PROFILE AND VEHICULAR RADIATED EMISSIONS

Consequences of the driving profile on real traffic vehicular radiated emissions are not analyzed in currently available automotive EMC standards like CISPR 16-2-3. The driving profile can be described by various parameters such as: vehicle velocity, linear acceleration, frontal inclination, regime engine, following distance, relative lane position, yaw angle, as well as position of throttle, clutch, and brake pedals [16].

In order to study the effect of the driving pattern on the corresponding radiated emissions of an electric vehicle in real traffic, experiments have to be carried out registering the driving profile signals as well as the corresponding radiated emissions of the vehicle under test (VUT). The problem isn't straightforward; because in real traffic, it is not possible to fix an onboard antenna to receive the radiated emissions due to the VUT only. This is because, this onboard antenna would receive radiated electromagnetic signals from other various sources like: radiated emissions due to other vehicles, Wifi, radio and television broadcast, mobile networks, satellite networks, Bluetooth devices, GPS, high voltage towers, ... etc.. Mainly for this reason, but also for the size and weight of the required antennas for this purpose, it's impossible to measure the real traffic vehicular radiated emissions due to a specific VUT. However, a lot of the signals related to the driver behavior can be easily measured by means of the vehicle's electronic system. Thus, the development of a model that would be able to estimate real traffic vehicular radiated emissions in terms of the corresponding driving profile signals would be a novel work. In this way, the relative change of the real traffic radiated emissions due to the driving pattern parameters can be quantified. Therefore, guidelines can be determined in order to ensure green driver behavior in terms of minimization of radiated electromagnetic interferences.

In order to tackle with this objective, authors propose a process of

three main stages as shown in Fig. 1. Firstly, tests with the vehicle in a semi-anechoic chamber have to be done measuring some driving profile signals as well as the corresponding radiated emissions. Secondly, artificial neural networks should be exploited to develop the desired model using data registered from the previous stage. Finally, real traffic experiments have to be done registering only the driving profile signals that would be simultaneously applied to the obtained model estimating the real traffic radiated emissions.

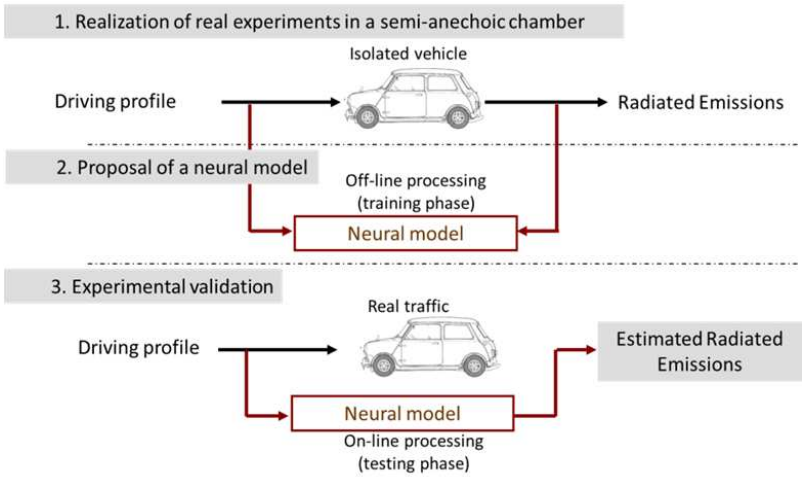

Figure 1. Complete process for estimating real traffic vehicular radiated emissions in terms of the driving profile.

As a first trial, the authors presented a measurement methodology of the radiated emissions of electric vehicles as well as the driving behavior [25]. This methodology is based on frequency domain EMI measurement procedure where a spectrum analyzer has been used to make sweeps of the radiated emissions signal without the capability of noise cancellation. In this paper, the authors propose a TDEMI measurement system employing an adaptive noise cancellation technique based on neural networks.

This paper describes the methodology and the obtained results of the first two stages of the complete process described in Fig. 1. That is, the velocity measurement of an electric motorcycle simultaneously with the corresponding radiated emissions in a semi-anechoic chamber. The motorcycle's speed has been controlled by a CAN bus connecting the motorcycle with a remote laptop outside the chamber. Adaptive noise cancellation techniques have been exploited to cancel out the electromagnetic noise due to the CAN bus. Once these data are

obtained, an MLP neural network is designed to model and estimate the electromagnetic emissions due to electrical vehicle under test operating in urban or interurban circuits.

3. METHODOLOGY

The key aspects of the methodology to evaluate the effect of the driving profile on the radiated electromagnetic emissions, based on TDEMI measurement, are shown in Fig. 2. EMI signals are captured by biconical antennas, filtered by anti-aliasing low pass filters, sampled as well as quantized by a digital oscilloscope, and sent to the PC's USB port via the GPIB/USB converter to be saved in a database for offline processing. The previous scenario is repeated until all the time domain records are saved in the PC's database. At the end of the experiment, the noise cancelation algorithm is applied. Then, spectra of the noisy, filtered, and CAN bus noise signals are computed via DFT. The measurement procedure is general, but an anti-aliasing filter with 32 MHz cutoff frequency has been used in this work; so the experimental results have been obtained up to 32 MHz range.

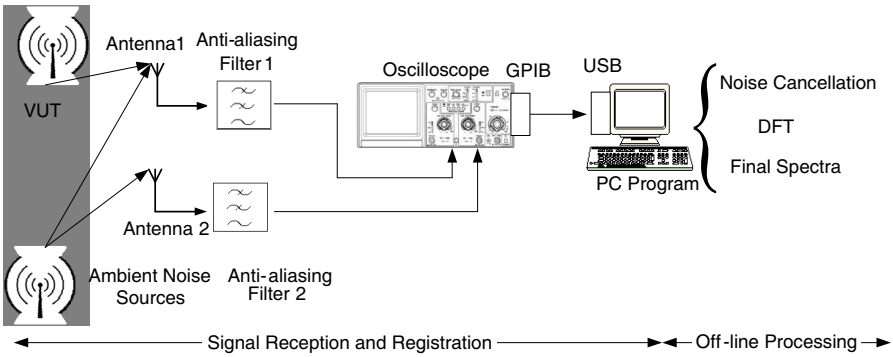

Figure 2. Block diagram of the proposed TDEMI measurement system.

The simultaneous registration of two antennas allows the off-line noise cancellation according to the adaptive noise cancellation theory. According to Fig. 2, antenna 1 is responsible for receiving the emissions of the VUT as well as the CAN bus noise, and antenna 2 captures only the CAN bus noise correlated with the noise component in the signal received by antenna 1. The frequency range of interest in the study must be covered by the antennas' bandwidth.

The following parameters of the oscilloscope have to be properly adjusted: sampling time T_s (or the sampling frequency F_s), capture

time T_c (i.e., duration of the time domain record of the oscilloscope), and recording time T_r (or the recording frequency F_r) [26, 27]. In this work, the EMI signals were sampled at 125 MHz, a 100 μs capture time has been selected, and a 250 ms recording time has been used.

Adaptive filtering techniques exploit the correlation between the noise component in the noisy EMI signal received by antenna 1, as can be seen in Fig. 2, and the reference noise signal received by antenna 2 to extract the EMI signal of the VUT. In this paper, a frequency domain FIR adaptive filter using the DFT filtering algorithm has been used. The filter's length is 4000 and the step size is 0.01. These parameters gave the best performance in terms of noise suppression.

Figure 3 includes two photos of a real test inside the semi-anechoic chamber of the University of Alcala in Spain. The overall system has been calibrated against a periodically calibrated spectrum analyzer (ESIB26) measuring a square waveform; because a square waveform theoretically has many odd harmonics; consequently covering all the measurement range. It's noteworthy that the absolute measurement accuracy is not a key point in this work; because the authors are interested in evaluating the relative change of the radiated emissions due to the driver behavior.

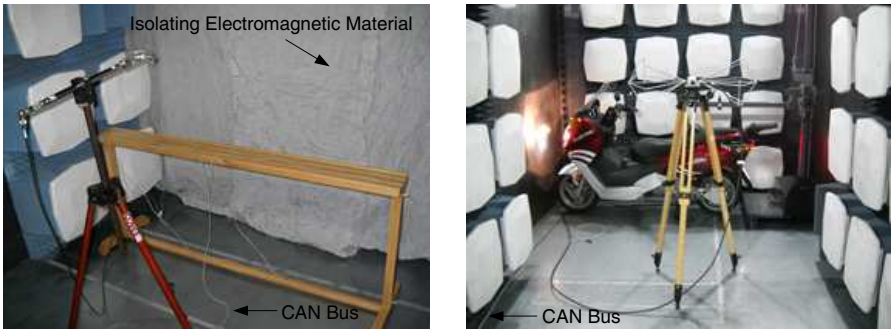

(a) (b)

Figure 3. Real photos of the measurement setup in the semi-anechoic chamber. (a) Isolating material and antenna 2. (b) Motorcycle and antenna 1.

4. NEURAL MODEL DEVELOPMENT

Various neural networks are available for function approximation. An MLP neural network, with "tansig" hidden neurons and linear output neurons, trained with backpropagation is chosen in this work because of its many useful function approximation properties [28]. It can

efficiently learn large data sets as compared to RBF and GRNN networks. Moreover, it has a relatively simple structure as compared to recurrent networks; where it doesn't contain neither delay elements nor feedback connections. Besides, the back-propagation training algorithm is already implemented in well-known software tools such as Matlab. And finally, an MLP network with sufficient hidden neurons can satisfy the universal approximation property [29].

Concerning the data preparation task, the early stopping technique is used to improve the generalization performance. In this technique the entire normalized data set has been divided randomly into training (80%), validation (10%), and testing (10%) subsets. The validation subset is employed during the training phase by monitoring the validation set error. It normally decreases during the initial phase of the training, as does the training set error. However when the network begins to over-fit the data, the validation set error begins to rise [30]. When it increases for 10 iterations, training stops and the network parameters are returned to the minimum validation set error state. The testing subset isn't used during training but the testing set error helps to compare different models based on the generalization performance.

Since the basic back-propagation learning algorithm is too slow for most practical applications, there have been extensive research efforts to accelerate its convergence. These researches fall into two categories, heuristic techniques and numerical techniques. In this paper, the MLP neural network is trained with the Levenberg-Marquardt numerical optimization method; because it is the fastest for function approximation problems of networks containing up to a few hundred weights [31].

When a particular training algorithm fails on an MLP network, it could be due to one of two reasons. The learning rule fails to converge to the proper values of the network parameters, perhaps due to unsuitable network initialization, or the inability of the given network to implement the desired function, perhaps due to an insufficient number of hidden neurons. To avoid the first possibility, each MLP neural network model was trained and tested 100 times. The network architecture with the lowest root mean square error (RMSE) on the testing data set has been chosen.

Concerning the second reason, there is no theory yet to explain how many hidden neurons are needed to approximate any given function. If there are too few hidden neurons, a high training error and high generalization error would result due to under-fitting. On the other hand, if there are too many hidden neurons, there would be a low training error, but there would still be a high generalization error

due to over-fitting. In most situations, there is no way to determine the best number of hidden neurons without training several networks and estimating the generalization error of each [29]. In this paper, the network growing technique [32] is applied by adding hidden neurons sequentially from 1 to 30 comparing the testing RMSE error.

Table 1. Complete process for estimating real traffic vehicular radiated emissions in terms of the driving profile.

Hidden neurons	5	10	15	18	25	30
Testing RMSE * 1e-11	0.2289	0.2229	0.2763	0.2097	0.2362	0.2266

Table 1 shows that 18 hidden neurons have achieved the best generalization performance in terms of the testing RMSE calculated as follows

$$\mathrm{RMSE} = \left[\frac{1}{N}\sum_{i-1}^{N}(p_i - Q_i)\right]^{1/2} \tag{1}$$

where O is the vector of observed (measured) values, P is the vector of model-estimated values, and N is the number of samples in the testing subset. The input to the neural network model is the vehicle velocity, while the output is the radiated emissions power. Therefore, this paper presents a single input single output neural network model whose structure is shown in Fig. 4.

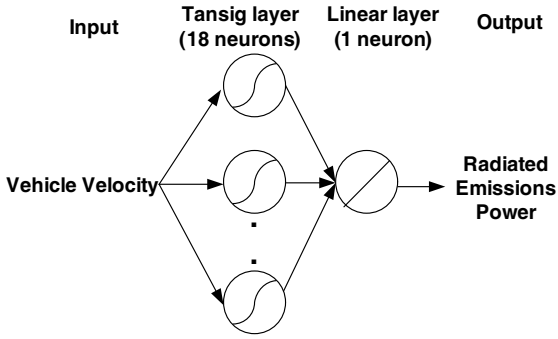

Figure 4. Structure of the proposed MLP model.

5. EXPERIMENTAL RESULTS

Before doing any radiated emission measurement, a test evaluating the background noise has been carried out in order to quantify the minimum detectable level. Then, the motorcycle was subjected to the typical Urban European Cycle (UEC) velocity profile depicted in Fig. 7. Fig. 5 shows the spectra of noisy (received by antenna 1), noise (received by antenna 2), and filtered (estimated by the adaptive noise canceller) signals. This figure clearly points out the capability of the proposed adaptive filter to cancel out or to reduce the additive CAN bus noise component on the motorcycle's EMI signal. For example, in the frequency ranges (1–2) and (7–8) MHz, although the reference CAN bus noise level was strong relative to the noisy signal level, the adaptive filter has successfully reduced the additive CAN bus noise.

Table 2 points out a comparison between the performance of different adaptive algorithms in terms of the root mean square difference (RMSD) between the noisy and estimated signals spectra. The more the RMSD, the more the capability of the adaptive noise canceler to reduce the additive CAN bus noise; because the RMSD in this case reflects the amount of noise suppression. As can be seen, the DFT adaptive algorithm achieved the best noise suppression performance in comparison with five different time as well as frequency domain adaptive algorithms.

Figure 6 shows the spectrogram of the filtered (estimated) EMI signal of the motorcycle in response to the applied velocity profile. It is clear that a part of the emission levels doesn't change with the velocity. However, there are frequency bands containing emission levels that relatively change with the corresponding UEC velocity profile.

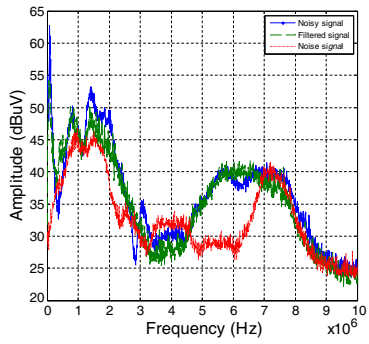

Figure 5. Peak detector spectra of noisy, noise, and filtered (estimated) signals.

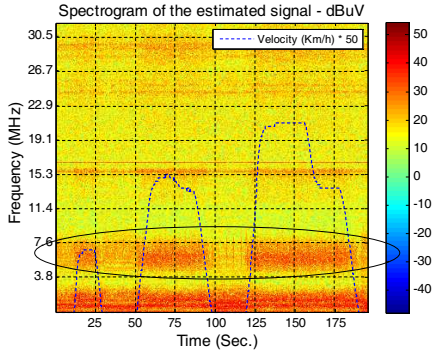

Figure 6. Spectrogram of the estimated motorcycle EMI signal (0–32 MHz).

Table 2. Comparison between different adaptive algorithms.

Algorithm & Parameters	RMSD
DFT[a] ($S^g = 0.01$)	4.3669
PBFD[b] ($S = 0.01$, BL[h] $= 100$)	3.8493
PBUFD[c] ($S = 0.01$, BL $= 250$)	1.0948
NLMS[d] ($S = 0.5$)	3.9104
SDLMS[e] ($S = 0.05$)	2.8912
SELMS[f] ($S = 0.5$)	4.0438

a: Discrete Fourier Transform [33]. *b*: Partitioned Block Frequency Domain [32]. *c*: Partitioned Block Unconstrained Frequency Domain [32]. *d*: Normalized Least Mean Square [33]. *e*: Sign Data Least Mean Square [34]. *f*: Sign Error Least Mean Square [34]. *g*: Step-size. *h*: Block Length.

An interesting frequency band is the one between 4.5 and 8 MHz, surrounded by an ellipse in Fig. 6.

According to Parseval's theorem, the sum (or integral) of the squares of a function is equal to the sum (or integral) of the squares of its transform. Consequently, the record mean power (RMP) has been calculated for all records in the (4.5–8) MHz frequency range according to (2), where N_{ss} is the number of FFT points in the record spectrum, i is the index of the FFT point in the record spectrum, and v is the value of the FFT point. Fig. 7 depicts the estimated and measured RMP as well as the applied UEC velocity profile. It clearly

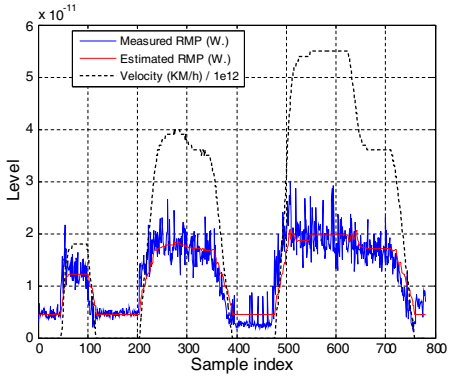

Figure 7. Estimated and measured RMP of the filtered motorcycle EMI signal (4.5–8 MHz band frequency) corresponding to the UEC velocity profile.

shows the direct relationship between the motorcycle's velocity and the corresponding RMP of the radiated emissions. The level of the RMP increases with increasing the motorcycle's velocity. Also, the level of the RMP remains at its minimum value when the motorcycle was not activated, i.e., the velocity was zero. Moreover, it shows that the developed MLP model can successfully estimate the radiated emissions RMP in terms of the applied vehicle velocity.

$$\mathbf{RMP} = \left(\frac{1}{N_{ss}} \sum\nolimits_{i=1}^{N_{ss}} v_i^2 \right) \Big/ 50 \tag{2}$$

6. CONCLUSIONS

Till now, the direct measurement of real traffic radiated emissions of electric vehicles is an unapproachable task. However the authors' proposal allows a reasonable estimation in terms of the driving profile applied to the vehicle, using artificial neural networks.

A methodology based on TDEMI measurement system has been developed to simultaneously register the radiated emissions as well as the velocity of electric motorcycles. An Urban European Cycle velocity profile has been remotely applied to the motorcycle under test by means of a CAN bus. The radiated emissions due to the CAN bus have been cancelled using frequency domain adaptive cancelling techniques.

Measurement results of real tests with a commercial electric motorcycle in a semi-anechoic chamber have been described and commented. The spectrogram of the estimated motorcycle radiated emissions showed that emission levels in a specific frequency range change directly with the motorcycle's velocity. An MLP neural network has been successfully trained and tested to estimate the radiated emissions RMP in terms of the corresponding vehicle velocity.

As a future work, authors intend to apply the developed ANN estimator to electric motorcycles in real traffic conditions, and to extend the neural model to other kinds of electric vehicles.

ACKNOWLEDGMENT

Authors would like to thank the cooperation of the High Technology and Homologation Center at the University of Alcala. This work has been funded by the Spanish Ministry of Science and Innovation through the SIGVE project (Ref. IPT-440000.2010-0020).

REFERENCES

1. Chan, C. C., "The state of the art of electric and hybrid vehicles," *Proceedings of the IEEE*, Vol. 90, No. 2, 247–275, 2002.
2. Guo, Y., L. Wang, and C. Liao, "Systematic analysis of conducted electromagnetic interferences for the electric drive system in electric vehicles," *Progress In Electromagnetics Research*, Vol. 134, 359–378, 2013.
3. Guttowski, S., et al., "EMC issues in cars with electric drives," *2003 IEEE International Symposium on Electromagnetic Compatibility*, Vol. 2, 777–782, 2003.
4. Gaul, H. W., T. Huettl, and C. Powers, "Radiated emissions testing of an experimental electric vehicle," *IEEE 1996 International Symposium on Electromagnetic Compatibility, Symposium Record*, 338–342, 1996.
5. Silva, F. and M. Aragon, "Electromagnetic interferences from electric/hybrid vehicles," *2011 XXXth URSI General Assembly and Scientific Symposium*, 1–4, 2011.
6. Mutoh, N., et al., "EMI noise control methods suitable for electric vehicle drive systems," *IEEE Transactions on Electromagnetic Compatibility*, Vol. 47, No. 4, 930–937, 2005.
7. Orimoto, H. and A. Ikuta, "Signal processing for noise cancellation in actual electromagnetic environment," *Progress In Electromagnetics Research*, Vol. 99, 307–322, 2009.
8. Lee, K.-C., J.-S. Ou, and M.-C. Fang, "Application of svd noise-reduction technique to PCA based radar target recognition," *Progress In Electromagnetics Research*, Vol. 81, 447–459, 2008.
9. Bieńkowski, P., K. Burnecki, J. Janczura, R. Weron, and B. Zubrzak, "A new method for automated noise cancellation in electromagnetic field measurement," *Journal of Electromagnetic Waves and Applications*, Vol. 26, No. 8–9, 1226–1236, 2012.
10. Frech, A., S. Braun, and P. Russer, "Time-domain EMI measurements in the presence of ambient noise," *IEEE International Symposium on Electromagnetic Compatibility, EMC*, 139–142, 2009.
11. Frech, A., S. Limmer, and P. Russer, "Noise cancelling algorithms for FPGA-based time-domain EMI measurements in real-time," *2011 IEEE International Symposium on Electromagnetic Compatibility (EMC)*, 484–488, 2011.
12. Dong, X. P., et al., "Detection and identification of vehicles based on their unintended electromagnetic emissions," *IEEE Transactions on Electromagnetic Compatibility*, Vol. 48, No. 4, 752–759, 2006.

13. Tsai, C. Y., E. J. Rothwell, and K. M. Chen, "Target discrimination using neural networks with time domain or spectrum magnitude response," *Journal of Electromagnetic Waves and Applications*, Vol. 10, No. 3, 341–382, 1996.
14. Atkins, R. G., R. T. Shin, and J. A. Kong, "A neural network method for high range resolution target classification," *Progress In Electromagnetics Research*, Vol. 4, 255–292, 1991.
15. Koroglu, S., N. Umurkan, O. Kilic, and F. Attar, "An approach to the calculation of multilayer magnetic shielding using artificial neural network," *Simulation Modelling Practice and Theory*, Vol. 17, No. 7, 1267–1275, 2009.
16. Aunchaleevarapan, K. P., W. Khan-Ngern, and S. Nitta, "Novel method for predicting PCB configurations for near field and far field radiated EMI using a neural network," *IEICE Trans. Commun.*, Vol. E86, No. B, 1364–1376, 2003.
17. Chahine, I., M. Kadi, E. Gaboriaud, A. Louis, and B. Mazari, "Characterization and modeling of the susceptibility of integrated circuits to conducted electromagnetic disturbances up to 1 GHz," *IEEE Transactions on Electromagnetic Compatibility*, Vol. 50, No. 2, 285–293, 2008.
18. Dangkham, P. S., S. Chaichana, K. Aunchaleevarapan, and P. Teekaput, "Recognition and identification of radiated EMI for shielding aperture using neural network," *PIERS Online*, Vol. 3, No. 4, 444–447, 2007.
19. Luo, M. and K.-M. Huang, "Prediction of the electromagnetic field in metallic enclosures using artificial neural networks," *Progress In Electromagnetics Research*, Vol. 116, 171–184, 2011.
20. Zaharis, Z. D., K. A. Gotsis, and J. N. Sahalos, "Adaptive beamforming with low side lobe level using neural networks trained by mutated boolean PSO," *Progress In Electromagnetics Research*, Vol. 127, 139–154, 2012.
21. Zaharis, Z. D., K. A. Gotsis, and J. N. Sahalos, "Comparative study of neural network training applied to adaptive beamforming of antenna arrays," *Progress In Electromagnetics Research*, Vol. 126, 269–283, 2012.
22. Li, X. and J. Gao, "Pad modeling by using artificial neural network," *Progress In Electromagnetics Research*, Vol. 74, 167–180, 2007.
23. Bermani, E., S. Caorsi, and M. Raffetto, "An inverse scattering approach based on a neural network technique for the detection of dielectric cylinders buried in a lossy half-space," *Progress In Electromagnetic Research*, Vol. 26, 67–87, 2000.

24. Espinosa, F., J. A. Jiménez, E. Santiso, A. Gardel, D. Pérez, J. Casanova, and C. Santos, "Design and implementation of a portable electronic system for vehicle-driver — Route activity measurement," *Measurement*, Vol. 44, No. 2, 326–337, 2011.
25. De Santiago, L., F. Espinosa, M. A. Ruiz, X. Jime, J. A. Nez, E. Santiso, D. Sanguino, A. Wefky, and W. G. Fano, "Effect of electrical vehicle-driver interaction on the radiated electromagnetic emissions: Measurement methodology," *2010 IEEE International Conference on Industrial Technology (ICIT)*, 1113–1118, 2010.
26. Keller, C. and K. Feser, "Fast emission measurement in time domain," *IEEE Transactions on Electromagnetic Compatibility*, Vol. 49, No. 4, 816–824, 2007.
27. Krug, F., D. Mueller, and P. Russer, "Signal processing strategies with the TDEMI measurement system," *IEEE Transactions on Instrumentation and Measurement*, Vol. 53, No. 5, 1402–1408, 2004.
28. Wefky, A. M., F. Espinosa, J. A. Jiménez, E. Santiso, J. M. Rodríguez, and A. J. Fernández, "Alternative sensor system and MLP neural network for vehicle pedal activity estimation," *Sensors*, Vol. 10, No. 4, 3798–3814, 2010.
29. Huang, G.-B., L. Chen, and C.-K. Siew, "Universal approximation using incremental constructive feedforward networks with random hidden nodes," *IEEE Transactions on Neural Networks*, Vol. 17, No. 4, 879–892, 2006.
30. Hagan, M. T., H. B. Demuth, and M. H. Beale, *Neural Network Design*, Pws Pub., 1996.
31. Hagan, M. T. and M. B. Menhaj, "Training feedforward networks with the Marquardt algorithm," *IEEE Transactions on Neural Networks*, Vol. 5, No. 6, 989–993, 1994.
32. Haykin, S. S., *Neural Networks: A Comprehensive Foundation*, Macmillan, 1994.
33. Haykin, S. S., *Adaptive Filter Theory*, Prentice Hall, 2002.
34. Bishop, C. M. and G. Hinton, *Neural Networks for Pattern Recognition*, Clarendon Press, 1995.